

# Preparation of Polymer/Graphite Conducting Nanocomposite by Intercalation Polymerization

GUO-HUA CHEN, DA-JUN WU, WEN-GUI WENG, WEN-LI YAN

Materials Science and Engineering College, Huaqiao University, Quanzhou 362011, China

Received 16 November 2000; accepted 29 December 2000

**ABSTRACT:** An *in situ* polymerization was conducted in the presence of expanded graphite obtained by rapid heating of the graphite intercalation compound (GIC) to form a polymer/expanded graphite conducting composite. Study showed that the graphite was dispersed in the form of nanosheets in the polymer matrix. The transition from an electrical insulator to an electrical semiconductor for the composite occurred when the expanded graphite content was 1.8 wt %, which was much lower than that of conventional conducting polymer composite. The composite exhibited high electrical conductivity of  $10^{-2}$  S/cm when the graphite content was 3.0 wt %. This great improvement of conductivity could be attributed to the high aspect ratio (width-to-thickness) of the graphite nanosheets. Study suggested that extensive rolling of the blend greatly affected the conductivity of the composite. © 2001 John Wiley & Sons, Inc. *J Appl Polym Sci* 82: 2506–2513, 2001

**Key words:** conducting polymer; expanded graphite; nanocomposite; intercalation

## INTRODUCTION

Blending polymer with conducting fillers including natural flake graphite, carbon black, and metal powder, to prepare electrically conducting composite has been investigated in the past few decades.<sup>1,2</sup> Loadings of filler needed for composite are usually as high as 15 wt % to reach a satisfactory conductivity, which results however, in the poor mechanical properties and the high density of the materials. Natural flake graphite (NG) is a very good electrical conductor with an electrical conductivity of  $10^4$  S/cm at room temperature and is naturally abundant.<sup>3</sup> Similar to the layer silicates such as montmorillonite, which has attracted great interest for the nanocomposites,<sup>4–6</sup>

natural flake graphite is also composed of nanolayers. Given the advantage of the high aspect ratios (width-to-thickness), montmorillonite once homogeneously dispersed in polymer matrix in nanosheets greatly improves the properties of the polymer and even generates new properties that cannot be derived from its counterparts. Could graphite materials be dispersed in polymer matrix like layered silicate? If it does, it would seem that a polymer/graphite composite with high electrical conductivity and low graphite loadings could be prepared. The objective of this work is to set an example process of fabricating a polymer/graphite nanocomposite via intercalation polymerization of monomers in the presence of expanded graphite.

Correspondence to: G.-H. Chen (hdcgh@hqu.edu.cn).  
Contract grant sponsor: National Natural Science Foundation of China; contract grant number: 29874016.

Contract grant sponsor: Natural Science Foundation of Fujian Province; contract grant number: 1999.

*Journal of Applied Polymer Science*, Vol. 82, 2506–2513 (2001)  
© 2001 John Wiley & Sons, Inc.

## EXPERIMENTAL

### Materials

The graphite used in this study was natural flake graphite with different diameters ranging from

50 to 1000  $\mu\text{m}$ , supplied from Shandong Qingdao Company (China). The monomers, styrene (St), and methyl methacrylate (MMA) were supplied by Shanghai Chemical Company (China). The monomers were purified by vacuum distillation before use. Concentrated sulfuric acid and concentrated nitric acid (c.p.) were used as chemical oxidizers to prepare expanded graphite. Benzoyl peroxide (BPO) was purified through recrystallization with  $\text{CHCl}_3$  and precipitant of  $\text{CH}_3\text{OH}$ .

### Preparation of Expanded Graphite

Expanded graphite was prepared following the methods reported in the literature.<sup>7,8</sup> A mixture of concentrated sulfuric acid and nitric acid (4 : 1, v/v) was mixed with graphite flakes (particle size 1000  $\mu\text{m}$ ), under appropriate cooling and stirring conditions. The reaction continued for about 16 h. The acid-treated natural graphite was washed with enough water to obtain treated graphite particles, which were then dried at 100°C to remove the remaining water by evaporation. The dried particles were heat treated at 1050°C for 15 s, thereby obtaining expanded graphite particles having *c*-direction expansions about 350 times that of the original *c*-direction dimension.

The same treatment of graphite flakes with a particle size of 60  $\mu\text{m}$  obtained a 20-fold expansion ratio.

### Intercalation and *in Situ* Polymerization

The expanded graphite made was mixed with St/MMA (70/30, v/v) in the presence of BPO (0.5 wt % to monomer) in a metal vessel that could be well sealed. The vessel was then heated at 150°C for 30 min and cooled to room temperature. A black solid was obtained.

The solid was crushed, rolled on a twin roller for 5 min, and then molded to get 120 × 60-mm<sup>2</sup> rectangle plates with a thickness of 4 mm.

### Characterization and Measurements

The volume conductivity of the nanocomposite samples was measured at room temperature by a GM-II automatic resistance tester (Research Institute for Carbon Materials, Shanxi, China) or DT 983 digital multimeter. Transmission electron microscopy (TEM) was obtained with a JEM-100 CXII TEM (Japan) using an acceleration voltage of 100 kV. Ultrathin samples of about 60 nm thickness were used. Scanning electron microscopy was obtained on an S-520 scanning electron

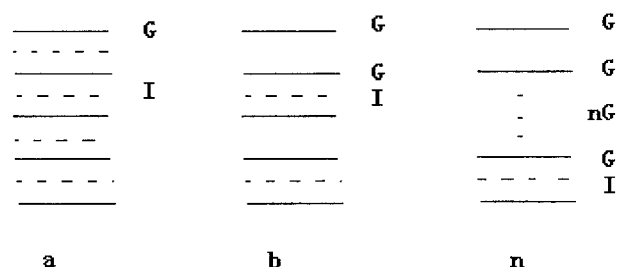


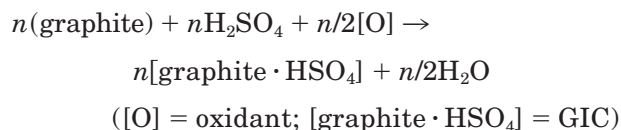
**Figure 1** Schematic illustration of the stage of GIC: solid line, graphite layer; dotted line, intercalated compound.

microscope (Hitachi, Japan). X-ray measurement used  $\text{CuK}_\alpha$  radiation, operated at 40 kV and 40 mA. Notched Izod impact strength was measured with an impact test machine (XCJ, Hebei, China) with the testing standard of Chinese GB1040-70. The tensile strength was tested on the XL-100 tensile tester (Guangzhou, China) with the testing standard of Chinese GB1040-70. The melt index was measured with an XZ-400 melt index tester (Jilin, China) at a temperature of 160°C.

## RESULTS AND DISCUSSION

### Exfoliation of the Graphite

Graphite is a form of carbon with the carbon atoms bonded in layers with weaker bonds of van der Waals forces between the layers. The weak interplanar forces allow intercalation by additional atoms or molecules that occupy spaces between the carbon layers. The interplanar spacing is thus increased.<sup>9,10</sup> Intercalation can be performed, for example, by immersing graphite flakes in concentrated nitric acid for a day or more. The reaction taking place between graphite and concentrated sulfuric acid and nitric acid can be expressed as follows:<sup>11,12</sup>



The resulting material, known as graphite intercalation compound (GIC) or intercalated graphite, comprises carbon layers and intercalated layers stacked on top of one another in a periodic fashion. The stacking can be of the form of Stage 1 [Fig. 1(a)], Stage 2 [Fig. 1(b)], or stage n [Fig. 1(n)], depending on the intercalation situation.

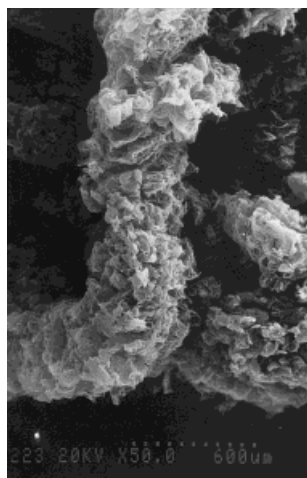


**Figure 2** SEM micrograph of expanded graphite.

Heating the GIC to a sufficiently high temperature causes exfoliation, which is a sudden increase in the dimension perpendicular to the carbon layers of the intercalated graphite, forming vermicular or wormlike shapes, known as expanded graphite. The exfoliated graphite flakes are expanded up to hundreds of times along the *c*-axis of the graphite. The original graphite flake of 20  $\mu\text{m}$  thickness may expand up to 2000–20,000  $\mu\text{m}$  in length (Fig. 2). Its density significantly decreases, whereas its electrical conductivity is not affected to a great degree.

#### Nanostructure of Exfoliated Graphite

The expanded graphite is a loose and porous vermicular material, whose structure is basically

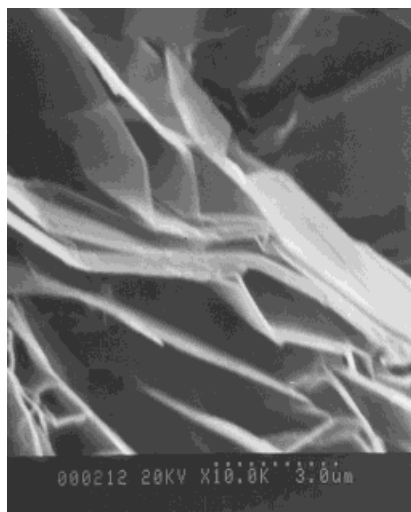


**Figure 3** SEM micrograph of expanded graphite.

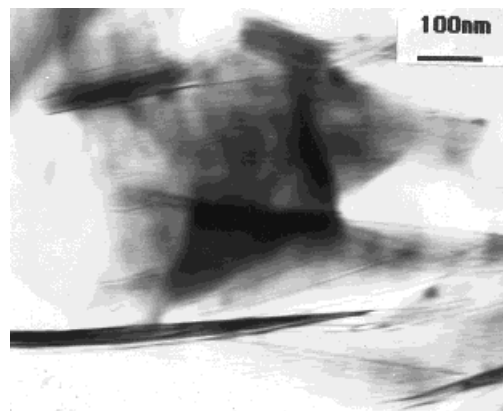


**Figure 4** TEM micrograph of poly(St-MMA)/expanded graphite without being rolled.

parallel boards, which collapse and deform desultorily, resulting in many pores of different sizes ranging from 10 nm to 10  $\mu\text{m}$ <sup>13,14</sup> (Fig. 3). The thickness of the graphite sheets in the exfoliated graphite found by SEM ranges from 100 to 400 nm. It seems hard to find the sheets with a thickness below 100 nm. Different sizes of graphite flake exhibited the same results in forming the expanded graphite, although their expansion ratio was different. According to the mechanism of the formation of the GIC and expanded graphite, the thickness of sheets in exfoliated graphite could be as thin as a single carbon layer, when its precursor GIC is in form of Stage 1. GICs prepared from chemical oxide intercalation are mostly in the form of Stages 1–5.<sup>15</sup> The thickness of the sheets comprising the vermicular graphite should be no larger than 2.5 nm, estimating the single carbon layer as 0.5 nm. The preceding statement was confirmed by TEM observation. Figure 4 shows that thinner sheets were found inside the exfoliated graphite. It reveals that thicker sheets found by SEM are composed of many thinner lamellae (nanosheets) with the thickness ranging from 10 to 40 nm (see Fig. 5).

The reason that SEM found no sheets thinner than 100 nm is possibly that nanosheets stack on

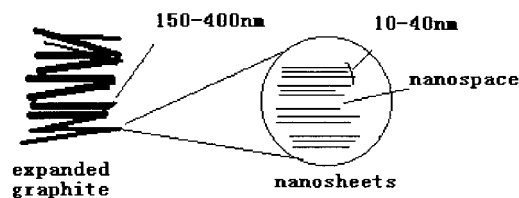


**Figure 5** Illustrative model for the expanded graphite, consisting of graphite nanosheets.

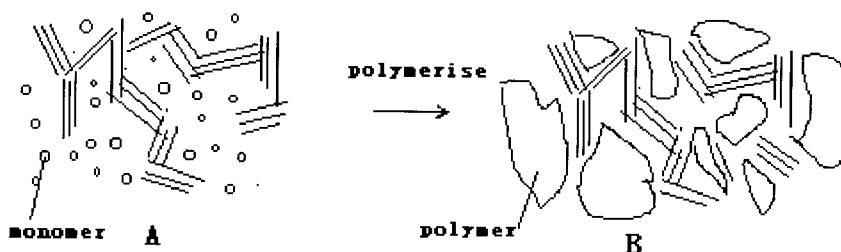


**Figure 6** Process of expanded graphite composite with polymer matrix via *in situ* polymerization.

each other or even fuse at the edge (surface) of the nanosheets (see Fig. 5). The edges of nanosheets possess such high surface energy that they were greatly affected and fuse into one at the high temperature of 1050°C.

### Nanostructure of the Composite

Figure 6 is a schematic illustration of the composite process of expanded graphite during *in situ* polymerization of monomers and rolled on a twin roller. The black lines represent the graphite sheets on the expanded graphite when they are viewed from a direction parallel to the sheets. The styrene (St) and methyl methacrylate (MMA) monomers and benzoyl peroxide (BPO) were intercalated into the nanospace of expanded graphite through physical adsorption of the porous expanded graphite during the mixing. The monomers St and MMA seem to have good affinity with graphite materials. They were quickly absorbed and reached an equilibrium state. The expanded graphite filaments in the solid prepared via *in situ* polymerization showed little difference from their pristine filaments by appearance. The X-ray diffraction (XRD) measurement (Fig. 7) confirmed that no significant change happened to the  $d$ -value and  $2\theta$  of 002 peaks between pure expanded graphite and the expanded graphite in the composite, indicating that no expansion happened to the gallery spaces of graphite carbon layers (graphite sheets). The expanded graphite showed broader for the 002 peak than that of the graphite flake, showing that the intercalation and exfoliation resulted in smaller size of graphite crystallite. The intercalation also widened the layer space from the  $d$ -value of 3.3670 Å for the graphite flake to 3.3732 Å for the expanded graphite. The intensities of 002 peaks for the expanded graphite sample were smaller than those of the graphite flake, ascribed to the fact that the amount of graphite crystallite in the expanded

graphite and in the composite were less than that in the graphite flake in the same volume sample. The unexpected smallness of the breadth of the 002 peak for the expanded graphite in composite possibly resulted from too little content of the expanded graphite in the sample (5.0%). The result is not coincident with Pan's report.<sup>16</sup>

The monomers or polymer intercalated into the gallery spaces of nanosheets instead of the gallery spaces of carbon layers of graphite. The intercalation of sulfuric acid and nitric acid did cause the expansion of the gallery of the graphite sheets, whereas the further addition of monomer or *in situ* polymerization of the monomers have no effect on the spacing of the gallery of the graphite carbon layers. The graphite sheets dispersed in

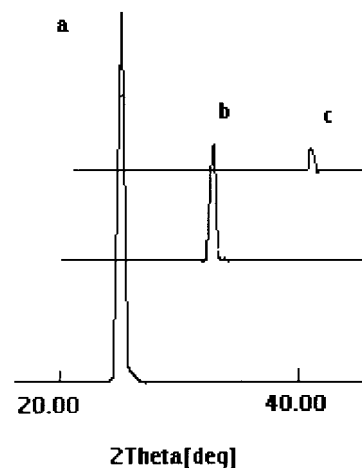


**Figure 7** X-ray diffraction curves of expanded graphite, poly(St–MMA)/expanded graphite, and the pristine graphite flake. (a) Graphite flake:  $2\theta$ , 26.450°; full width at half maximum (FWHM), 0.235;  $d$ -value, 3.3670 Å; intensity, 25,129. (b) Expanded graphite:  $2\theta$ , 26.400°; FWHM, 0.294;  $d$ -value, 3.3732 Å; intensity, 8499. (c) Polymer/expanded graphite (5 wt %):  $2\theta$ , 26.350°; FWHM, 0.176;  $d$ -value, 3.3795 Å; intensity, 578.

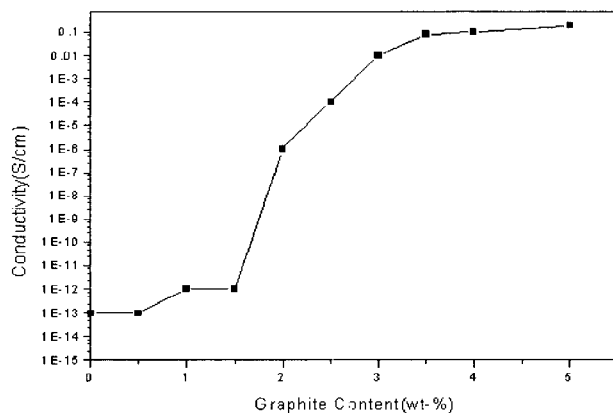


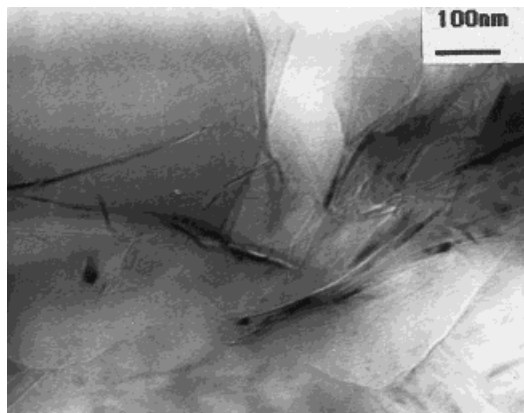
**Figure 8** Electrical conductivity of poly(St-MMA)/expanded graphite as a function of the graphite content.

the final polymer matrix had a thickness of about 20 nm, revealing that they comprise about 40 carbon layers.

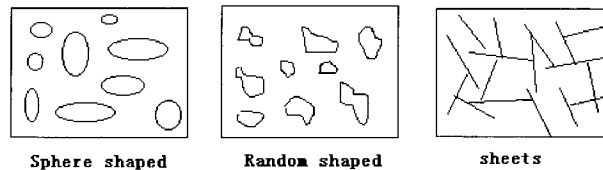
### Electrical Conductivity

Figure 8 shows the variation of the volume electrical conductivity of poly(St-MMA)/graphite nanocomposites as a function of the graphite content. Like most polymers, poly(St-MMA) is not electrically conductive and its room temperature volume conductivity in a dry state is no higher than  $10^{-14}$  S/cm. The addition of graphite greatly improved its conductivity with a sharp transition from an electrical insulator to an electrical semiconductor. The percolation threshold value of the conducting composite is about 1.8 wt % of expanded graphite, which is much lower than that of conventional conducting composites.<sup>1,17</sup>

Figure 9 shows the TEM photomicrographs of



**Figure 9** TEM micrograph of poly(St-MMA)/graphite nanocomposite.



**Figure 10** Schematic illustration of the effect of geometry of fillers on the formation of a conducting network.

poly(St-MMA)/expanded graphite. The solid lines correspond to exfoliated graphite sheets viewed from their side direction, whereas the domains are the poly(St-MMA) matrix. Apparently, graphite sheets in the polymer matrix had a thickness of 10–20 nm. The dispersion of the graphite sheets was relatively homogeneous in most parts of the matrix, although there are still some graphite sheets existing in micrometer particles.

The percolation threshold for the electrical conductivity depends very much on the geometry of the conducting filler. Filler with a higher aspect ratio, such as sheetlike or fiberlike filler, has an advantage in forming the conducting network in polymer matrix than that of filler in either round or ellipse shape, which has a lower aspect ratio (Fig. 10). For a given content of filler, the percolation threshold is lower for a sheetlike one than that for a spherical one. This is the main reason that the percolation threshold of the poly(St-MMA)/graphite nanocomposite is much lower than that of a conventional composite such as carbon black composite.

For the poly(St-MMA)/expanded graphite system, graphite flakes were dispersed in the matrix in nanoscale sheets (Fig. 9). The graphite nanosheets in the matrix formed the conducting network with low content.

The electrical conducting property and the structure of the composite were greatly affected by the process of being rolled. The beginning solid prepared from *in situ* polymerization exhibited the highest conductivity of about  $10^{-1}$  S/cm when the content of the expanded graphite was 3.0 wt %, although it decreased gradually when rolled on the twin roller at beginning stage and decreased sharply later in the rolling process (Fig. 11). The reason for the decline of the conductivity is possibly that the conducting network in the composite was destroyed during the rolling process.

Figure 12 shows a schematic illustration of the structural change of the poly(St-MMA)/expanded

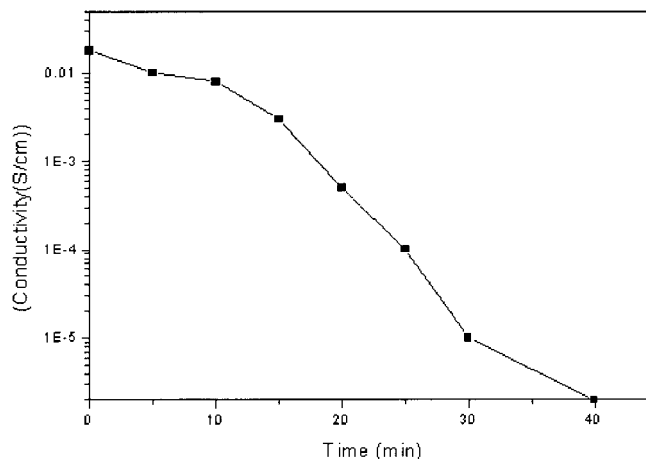


**Figure 11** Dependency of the electrical conductivity on the time of being rolled.

graphite composite during the rolling process. The ordered or disordered solid lines represent the graphite sheets viewed from a direction parallel to the planes of the sheets. The B product in Figure 12 was directly prepared via *in situ* polymerization (see also Fig. 6). The expanded graphite sheets in the composite contact each other very well, forming a conducting network with excellent conducting property. After being properly rolled, expanded graphite were better dispersed in the matrix with only a little disruption (in structure C, the polymer is omitted) and its conductivity is still high for the composite. When the composite is rolled extensively, a large amount of expanded graphite or even the graphite sheets will be broken (Fig. 12, structure D) and the conductivity of the composite significantly decreased. Continued

rolling of the composite would result in significant breaking of the graphite sheets, forming the dispersion structure as in structure E of Figure 12, which has very poor conducting properties. TEM investigation has confirmed the speculation (Fig. 13). The ideal dispersion is shown in Figure 12, structure F, although it is not easy to achieve.

### Mechanical Properties

Figure 14 shows the dependency of the tensile strength of poly(St-MMA)/expanded graphite on the graphite content in the matrix. The tensile strength of the composite was a little higher than that of the pure polymer, as expected. The presence of rigid graphite sheets increased the tensile modulus of the polymer matrix. The graphite sheets seemed to act as a reinforcing filler to the polymer matrix.

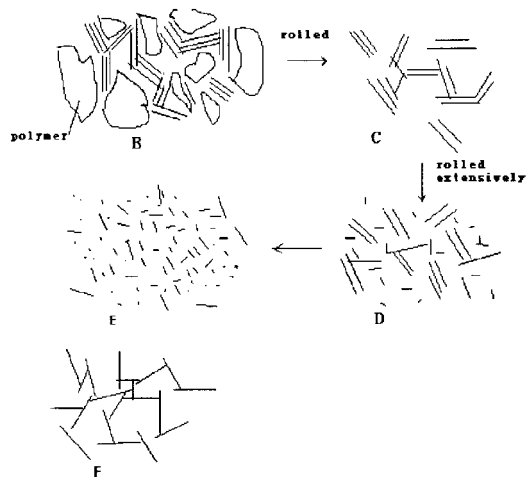


**Figure 12** Schematic illustration of the composite's change of structure during the rolling process.

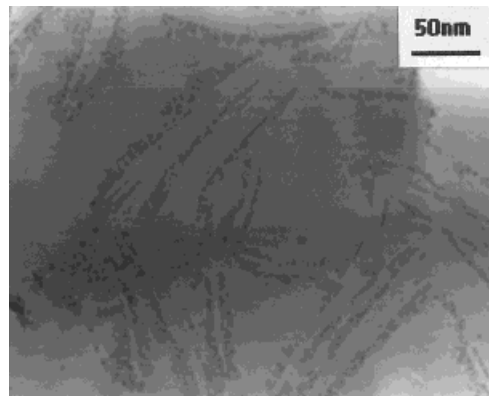


**Figure 13** TEM micrograph of poly(St-MMA)/expanded graphite after being thoroughly rolled.

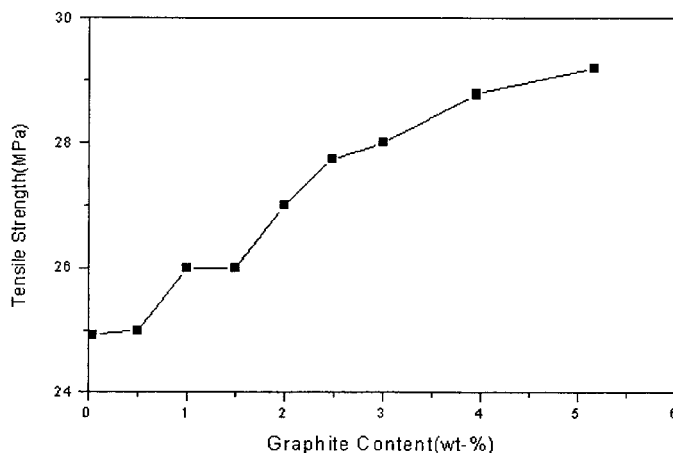


**Figure 14** Dependency of the tensile strength of poly(St-MMA)/expanded graphite on the graphite content.

Figure 15 shows the notched Izod impact strength of poly(St-MMA)/expanded graphite as a function of the graphite content. The composite displayed a gentle reduction in notched impact strength with increasing graphite content from 0.5 to 3.0 wt %, a sharp reduction when graphite content was more than 3.0 wt %, which would imply that the dispersion of graphite sheets in the matrix is more homogeneous when its content is lower. Figure 16(a) shows that the melt index of the composite increased with the graphite content at a range of 0–3.0 wt % and decreased when the graphite content was more than 3.0 wt %. The increase of the mobility of the composite was mainly caused by the thorough dispersion of the graphite and the lubricity of the graphite. When the graphite was more than 3.0 wt %, the disper-

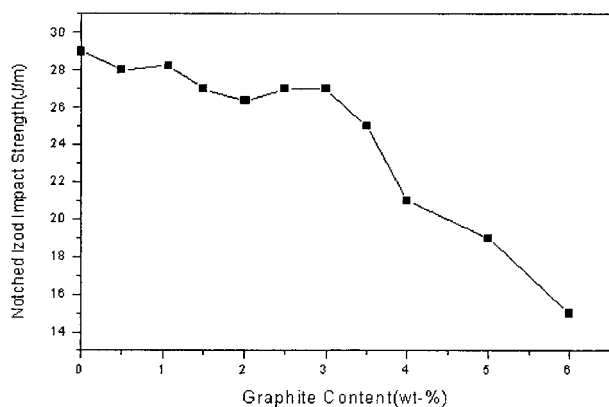


**Figure 15** Dependency of the notched Izod impact strength of poly(St-MMA)/expanded graphite on the graphite content.

sion became poor. Figure 16(b) shows that the melt index of the composite was higher after being well rolled. Evidently, the mobility of the composite strongly depended on the dispersion of the graphite.

The result would also support the speculation that the reason for the decrease of the notched Izod impact strength when the graphite content went beyond 3.0 wt % was attributed to the poor dispersion of the graphite. Although higher notched Izod impact strength could be achieved by extensive rolling of the composite, the electrical conductivity would be sacrificed. Further investigation will focus on the influence of processing technology on the dispersion of the graphite, the mechanical properties, and the conductivity of the composite.

## CONCLUSIONS

A process of *in situ* polymerization of styrene and methyl methacrylate in the presence of expanded graphite was developed to fabricate an electrically conductive polymer/graphite nanocomposite. Expanded graphite was shown to be a good conducting filler for polymers. The percolation threshold of the graphite for the electrical conductivity at room temperature was 1.8 wt %, which was much lower than that for conventional conducting polymer composites. The electrical conductivity reached  $10^{-2}$  S/cm at a graphite content of 3.0 wt %. The graphite nanosheets with high aspect ratio (width-to-thickness) in the expanded graphite played an important role in lowering the

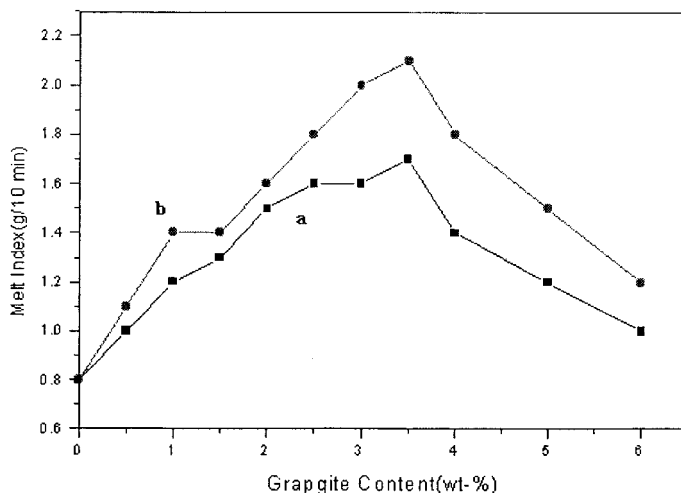


**Figure 16** Dependency of the melt index of poly(St-MMA)/expanded graphite on the graphite content: (a) samples rolled for 5 min; (b) samples rolled for 30 min.

transition threshold of the graphite content. Extensive rolling strongly affected the conductivity of the composite.

## REFERENCES

- Saunders, D. S.; Galea, S. C.; Deirmendjian, G. K. *Composite* 1993, 24, 309.
- Bennett, C. H. *J Appl Phys* 1972, 43, 2929.
- King, J. A.; Tucker, K. W.; Vogt, B. D. *Polym Compos* 1999, 20, 643.
- Usuki, A.; Kojima, Y.; Kawasumi, M.; Okada, A.; Fukushima, Y. *J Mater Res* 1993, 8, 1179.
- Giannelis, E. P. *Adv Mater* 1996, 8, 29.
- Lebaron, P. C.; Wang, Z.; Pinnavaia, T. *J Appl Clay Sci* 1999, 15, 11.
- Nakajima, T.; Matsuo, Y. *Carbon* 1994, 32, 469.
- Hérol, A.; Petitjean, D.; Furdin, G.; Klatt, M. *Mater Sci Forum* 1994, 152/153, 281.
- Ruisinger, B.; Boehm, H. P. *Carbon* 1993, 31, 1131.
- Shioyama, H.; Tatsumi, K. *Tanso (Jpn)* 1993, 15, 207.
- Nishimura, T. *Macromol Chem Rapid Commun* 1980, 1, 573.
- Hashimoto, K.; Sumitomo, H.; Kowasumi, M. *Polym Bull* 1984, 11, 121.
- Chung, D. D. L. *J Mater Sci* 1987, 22, 4190.
- Chuan, X.-Y.; Zhang, C. D.; Zhou, X.-R. *Carbon* 1997, 35, 311.
- Aronson, S.; Frishberg, G.; Frankl, G. *Carbon* 1971, 9, 715.
- Pan, Y.-X.; Yu, Z.-Z.; Ou, Y.-C.; Hu, G.-H. *J Polym Sci Part B Polym Phys* 2000, 38, 1626.
- Celzard, A.; Furdin, G.; Mareche, J. F.; McRae, E. *Solid State Commun* 1994, 92, 377.